RESEARCH

Isolation and Expression Analysis of *CYP9A11* and Cytochrome P450 Reductase Gene in the Beet Armyworm (Lepidoptera: Noctuidae)

Chunqing Zhao,[1,2,*] Xiaoyun Feng,[1,*] Tao Tang,[1,3] and Lihong Qiu[1,4]

[1]College of Science, China Agricultural University, Beijing, China
[2]College of Plant Protection, Nanjing Agricultural University, Nanjing, China
[3]Institute of Plant Protection, Hunan Academy of Agricultural Sciences, Changsha, China
[4]Corresponding author, e-mail: lihongqiuyang@126.com
*These authors contributed equally to this work.

Subject Editor: Daniel Swale

J. Insect Sci. *(2015)* 15(1): 122; DOI: 10.1093/jisesa/iev100

ABSTRACT. Cytochrome P450 monooxygenases (CYPs), as an enzyme superfamily, is widely distributed in organisms and plays a vital function in the metabolism of exogenous and endogenous compounds by interacting with its obligatory redox partner, CYP reductase (CPR). A novel CYP gene (*CYP9A11*) and *CPR* gene from the agricultural pest insect *Spodoptera exigua* were cloned and characterized. The complete cDNA sequences of *SeCYP9A11* and *SeCPR* are 1,931 and 3,919 bp in length, respectively, and contain open reading frames of 1,593 and 2,070 nucleotides, respectively. Analysis of the putative protein sequences indicated that *Se*CYP9A11 contains a heme-binding domain and the unique characteristic sequence (SRFALCE) of the CYP9 family, in addition to a signal peptide and transmembrane segment at the *N*-terminal. Alignment analysis revealed that *Se*CYP9A11 shares the highest sequence similarity with CYP9A13 from *Mamestra brassicae,* which is 66.54%. The putative protein sequence of *Se*CPR has all of the classical CPR features, such as an *N*-terminal membrane anchor; three conserved domain flavin adenine dinucleotide (FAD), flavin mononucleotide (FMN), and nicotinamide adenine dinucleotide phosphate (NADPH) domain; and characteristic binding motifs. Phylogenetic analysis revealed that *Se*CPR shares the highest identity with *Ha*CPR, which is 95.21%. The *SeCYP9A11* and *SeCPR* genes were detected in the midgut, fat body, and cuticle tissues, and throughout all of the developmental stages of *S. exigua*. The mRNA levels of *SeCYP9A11* and *SeCPR* decreased remarkably after exposure to plant secondary metabolites quercetin and tannin. The results regarding *SeCYP9A11* and *SeCPR* genes in the current study provide foundation for the further study of *S. exigua* P450 system.

Key Words: *Spodoptera exigua*, cytochrome P450, CYP9A11, CPR, expression

The beet armyworm *Spodoptera exigua* (Hübner) (Lepidoptera: Noctuidae) is an economically important insect that is responsible for damaging a wide range of crops throughout the world, including the United States (Atkins 1960; Ruberson et al. 1994), Europe (Mohaghegh et al. 2001), and Asia (Cheng et al. 1988; Park et al. 1991). *Spodoptera exigua* has received increased attention partly due to insecticide resistance, which has been widely documented (Ruberson et al. 1994; Che et al. 2013).

Enzymatic detoxification is considered a major mechanism of insecticide resistance. Cytochrome P450 monooxygenase (CYP), as the most prominent metabolic oxidase (Bergé et al. 1998; Scott et al. 1998; Scott 1999), can generate an effective catalytic cycle by interacting with NADPH-CYP reductase (CPR, EC 1.6.2.4) and other partners in the CYP pathway. Meanwhile, as the primary redox partner of CYPs, CPR mainly shuttles electrons from NADPH to known CYPs (Wang et al. 1997) and is hypothesized to be the limiting factor for the CYP catalytic process (Pompon et al. 1996). CPR plays an important role in the metabolism of drugs and steroids in *Homo sapiens* as well (Riddick et al. 2013). Konus et al. (2013) has pointed out that CYP process in insecticide metabolism requires CPR for electron transfer. CYP interacts with CPR in insect microsomes, where the ratio of CYP to CPR is suggested to be ∼6–18 to 1 (Feyereisen 2012). Several studies have varied the ratio of CYP and CPR in reconstituted systems to better understand the activity of the system (Wen et al. 2003; Mao et al. 2006; Murataliev et al. 2008). However, understanding of the interaction between CYP and CPR in insects is still limited. To better understand the CYP and CPR in *S. exigua,* in this study, novel *CYP* and *CPR* genes from *S. exigua* were cloned and characterized. And the mRNA expression levels were measured to determine the tissue distribution, levels throughout developmental stages and effects of quercetin and tannin. The results of the current study are expected to enrich the knowledge of P450 enzyme systems and assist in the elucidation of the functions of P450 and CPR in *S. exigua*.

Materials and Methods

Insect. A colony of beet armyworm was collected from Hebei Province of China in 1988, and the larvae were reared with the artificial diet without exposure to any insecticide at 27 ± 1°C and 75–80% relative humidity under a 16: 8 (light: dark) photoperiod. The eggs were sterilized with a 0.1% sodium hypochlorite solution, and the moths were supplied with a 5% honey solution as a nutrient.

RNA Extraction and cDNA Synthesis

Total RNA was extracted successively with a SV Total RNA Isolation System (Promega, WI), quantified using a Lambda Bio 40 UV spectrophotometer (Perkin Elmer Company, MA), and treated using RQ1 RNase-Free DNase (Promega) to remove the residual genomic DNA. The cDNA was synthesized using the EasyScript Two-Step reverse transcription polymerase chain reaction (RT-PCR) SuperMix Kit (TransGen Biotech, Beijing, China) with treated total RNA from seven developmental stages (including the whole worm of 1st to 5th instar larvae, pupae, and moth) and from the cuticle, fat body, and midgut tissues of fifth instar larvae. For 5′- and 3′-rapid amplification of cDNA ends (RACE), cDNA was synthesized using the SMARTer RACE cDNA Amplification Kit (Clontech Laboratories Inc., Dalian, China) following the kit manual.

Molecular Cloning of the Putative P450 Gene from S. exigua. The full-length cDNA of *SeCYP9A11* was obtained with RT-PCR and RACE techniques. The degenerate primers, DCYP1 and DCYP2 (Table 1), were designed on the basis of highly conserved amino acid

Table 1. Primers used in this study

Function	Primer set	Primer sequence (5′→3′)
Degenerate PCR	DCYP1	TYGCYGGHYWYGAVAC
	DCYP2	CCDATRCARTTBCKDKGHCC
	DCPR1	GTGGGRCARGGGAATGGRTG
	DCPR2	TAYGGYGARGGMGATCCCAC
5′-RACE	CYP3	TTGCCACTGTGCTTCACGTCATGTTCT
	TCPR2	GGTCCATGAGTTACAAGACGGAACTGACG
Provided by kit	UPM	CTAATACGACTCACTATAGGGCAAGCAGTGGTATCAACGCAGAG
3′-RACE	CYP4	CACCGCGATCCTCAGTACTTCCCAG
	TCPR1	ATGAAGCTGGTGATCATGTGGCTGTG
Amplification of cDNA fragment	CYP5	CCTCCATCGTAATCCTGAATACTTCCC
	CYP6	TCCCTAACCCTACAAAGTTCGACCCGG
	TCPR8	CGCCACTCACAGAACATAACAC
	TCPR10	TGTAAAGTCCTCTCGAAAAATA
RT-qPCR analysis	qCYP1	GGATCTTACAACTCGCTACGC
	qCYP2	TTGCTGCTGTCCTACCCATTA
	qTCPR3	TGCAAAGTCAAACCCCCATT
	qTCPR4	GCTCATATTTCTCAAGTTCCTCCTG
House-keeper gene	F-β-Actin	TCCTCCGTCTGGACTTGGC
	R-β-Actin	CCTTGATGTCACGCACGATTT

M=A/C, R=A/G, W=A/T, S=G/C, Y=C/T, K=G/T, V=A/G/C, H=A/C/T, D=A/G/T, B=G/C/T, N=A/G/C/T

sequences (DCYP1: AGFET and DCYP2: GPRNCIG) of the first helix and the heme binding domain of CYPs in several species, respectively. The thermal cycle was followed: 3 min at 94°C, 35 × (30 s at 94°C, 30 s at 47°C, and 2 min at 72°C), and 10 min at 72°C. A fragment of ∼480 bp (Supp Fig. 1 [online only]) was amplified, gel-purified using a Wizard SV Gel and PCR Clean-Up System (Promega), ligated into the pGEM-T vector (Promega) and then transformed into *Escherichia coli* Top10 cells (TransGen Biotech). The transformants were screened on LB-agar plates containing 60 μg/ml of ampicillin. The positive clones were cultured and then sequenced by Invitrogen Company (Life Technologies, Shanghai, China).

After partial putative DNA confirmation was obtained by homology searching in National Center for Biotechnology Information (NCBI) and by Basic Local Alignment Search Tool (BLAST) analysis, the corresponding specific primers CYP3 and CYP4 (Table 1) for 5′- and 3′-RACE of cDNA were designed, respectively. The putative 5′- and 3′-RACE fragments were overlapped and identified as the 5′- and 3′-end of the putative *SeCYP9A11* gene after sequencing. Subsequently, the open reading frame (ORF) of *SeCYP9A11* cDNA was amplified by PCR using specific primers CYP5 and CYP6 (Table 1). The PCR program was followed: 1 min at 95°C, 40 × (20 s at 95°C, 20 s at 55°C, and 1 min at 72°C), and then 5 min at 72°C.

Molecular Cloning of the Putative SeCPR Gene. Based on the highly conserved amino acid sequences region (DCPR1: YGEDPTDN and DCPR2: HPFPCPT, boxed in Supp Fig. 4 [online only]) of CPR, known from other CPR sequences, primers DCPR1 and DCPR2 (Table 1) were designed to clone partial fragment of *SeCPR* gene. The PCR procedure was followed initial denaturation (95°C, 5 min); 35 cycles (95°C, 30 s; 45°C, 30 s; and 72°C, 1 min); and elongation (72°C, 10 min). Based on the partial fragment of *SeCPR* gene, the specific primers for 5′-RACE (TCPR2) and 3′-RACE (TCPR1) were designed, respectively, and the corresponding cDNAs were obtained with the RACE technique. The full-length ORF of *SeCPR* was cloned by specific primers (TCPR8 and TCPR10).

Sequence Analysis of SeCYP9A11 and SeCPR. The full-length cDNAs and the deduced amino acid sequences of *SeCYP9A11* and SeCPR were determined with the DNAMAN 6.0 software (Lynnon Biosoft, Quebec, Canada). The sequence similarities were compared using the DNAMAN 6.0 software with homologous sequences from NCBI. The theoretical *iso*-electric point (*pI*) and molecular weight (Mw) were calculated with the Compute pI/Mw (http://web.expasy.org/compute_pi/) (Gasteiger et al. 2005). The signal-peptides of *SeCYP9A11* and *SeCPR* were predicted by the SignalP 4.0 server (http://www.cbs.dtu.dk/services/SignalP/) (Petersen et al. 2011).

The secondary structure, binding domains, and catalytic residues of *SeCYP9A11* and *SeCPR* were predicted by PHYRE2 Protein Fold Recognition Server (http://www.sbg.bio.ic.ac.uk/phyre2/html/) (Kelley and Sternberg 2009), and the conserved domains were searched on the NCBI website (http://www.ncbi.nlm.nih.gov/Structure/cdd/wrpsb.cgi) (Marchler-Bauer et al. 2011). The transmembrane domains were analyzed by the TMHMM Server 2.0 (http://www.cbs.dtu.dk/services/TMHMM-2.0/) (Krogh et al. 2001). The hydrophilicity were predicted using Hphob. / Kyte & Doolittle with ProtScale (http://web.expasy.org/protscale/) (Gasteiger et al. 2005). The phylogenetic tree was constructed by MEGA 5.0 using the default settings and neighbor-joining method (http://www.megasoftware.net/) (Tamura et al. 2011).

The *SeCPR* protein was deduced using the I-TASSER server (http://zhanglab.ccmb.med.umich.edu/I-TASSER/) on basis of the rat (*Rattus norvegicus*) CPR (PDB: 1AMO) (Yang et al. 2015). The corresponding PDB file of the highest ranking model comparing to the *R. norvegicus* CPR was modified and labeled using UCSF Chimera software (http://www.cgl.ucsf.edu/chimera/) (Pettersen et al. 2004).

Expression Levels of SeCYP9A11 and SeCPR mRNAs in Response to Secondary Plant Substances. Quercetin was used at doses of 0.1 and 1 mg/g (W/W, weight of test chemical/weight of artificial diet), and tannin was used at doses of 0.5, 1, and 5 mg/g (W/W). The fourth instar larvae were selected and starved for 12 h before being fed an artificial diet mixed with quercetin or tannin at different doses. Total RNA from the *S. exigua* midgut was extracted at 48 h after treatment and then purified with the SV Total RNA Isolation System. The cDNAs were synthesized and used to detect the expression levels of *SeCYP9A11* and *SeCPR* mRNA by RT-qPCR method.

RT-qPCR Analysis of SeCYP9A11 and SeCPR. Equal quantities of total RNA for both genes were reverse transcribed by the EasyScript Two-Step RT-PCR SuperMix. The RT-qPCR reaction system contained 10 μl of a 2×Ultra SYBR Mixture (with ROX) (CWBiotech, Beijing, China), 0.3 μl of each gene-specific primer (qCYP1 and qCYP2 or qTCPR3 and qTCPR4, Table 1) for a final concentration of 1 μM, 2 μl of cDNA template, and 7.4 μl of RNase-free water. The amplification was performed at 95°C for 10 min and followed by 40 cycles (95°C for 15 s and 62°C for 1 min). Each sample reaction was carried out in triplicate, and the dissociation curve analysis of the amplified products was

performed at the end of each PCR reaction to confirm the specificity and unique of the PCR product. The cycle threshold (Ct) values of *SeCYP9A11*, *SeCPR,* and the β-actin were examined and the comparative Ct method was used to analyze the expression of *SeCYP9A11* and *SeCPR* mRNA as described by Livak et al. (2001). RT-qPCR data were analyzed with SDS 1.4 software (Applied Biosystems, CA).

Statistical Analyses. Values were shown as the mean ± SE of triplicates using one-way ANOVA and the significant differences were analyzed using the SPSS statistics program (SPSS Inc., IL) with Duncan's new multiple range tests (DMRT). A P value < 0.05 was considered statistically significant. The figures were generated with GraphPad Prism 5.0 (GraphPad Software Inc., CA).

Results

Sequence Analysis of SeCYP9A11 Gene. The full-length cDNA of *SeCYP9A11* was verified after assembling the sequences of ~480, ~500 and ~1,500 bp from the degenerate PCR, 3′- and 5′- RACE PCR, respectively (Supp Fig. 1A [online only]) and then deposited in the GenBank database with accession number of **HQ340240.1**. The complete sequence of *SeCYP9A11* contains a 196 bp 5′-untranslated region (5′-UTR), a 142 bp 3′-UTR with a poly-A nucleotide sequence and the 1,593 bp ORF, which encodes a putative protein of 530 amino acids with a predicted Mw of 61.61 kDa and a theoretical *pI* of 8.10.

A signal peptide (Supp Fig. 2A [online only]) and a transmembrane helix (data not shown) were predicted in the *Se*CYP9A11. The *Se*CYP9A11 exhibited the important characteristics and common structural features of CYP superfamily members. The consensus sequences [XGX(D/E)T] within the I-helix region (AGFET) and the heme-binding domain (FXXGXRXCXG) in the C-terminal region (FGVGPRNCIG) were found in the *Se*CYP9A11 sequence (Fig. 1). The unique CYP9-family characteristic motif [SR(F/I/L)(A/G)XX(Q/E)] was also observed in *Se*CYP9A11 (SRFALCE, Fig. 1) and the hydrophobicity prediction of *Se*CYP9A11 is shown in Supp Fig. 3A [online only]. The secondary structures, such as the I-helix, Ca-helix, K-helix, and heme-binding domain, were predicted in the primary structures of *Se*CYP9A11 as well (Fig. 1).

The deduced amino acid sequences of *Se*CYP9A11 shared 66.54% identity with CYP9A13 from the cabbage moth (*M. brassicae*), 65.73% with CYP9A18, and 65.23% with CYP9A12 from the cotton bollworm (*Helicoverpa armigera*), 62.27% with *Se*CYP9A9, and 59.10% with CYP9A19 from both the silkworm (*Bombyx mandarina* and *Bombyx mori*) (Fig. 2A).

Sequence Analyses of SeCPR Gene. After RT-PCR and RACE-PCR, three cDNA fragments, including the ~700 bp fragment from the degenerate primers, the ~2,700 bp from the 5′ RACE, and the ~1,200 bp from the 3′ RACE, were amplified using degenerate and specific primers (Supp Fig. 1B [online only]). The full-length cDNA sequence was obtained after assembling the three fragments and then deposited in the GenBank database with accession number **HQ852049.1**. The complete sequence of *SeCPR* contains a 195-bp 5′-UTR and a 1,648-bp 3′-UTR with a canonical polyadenylation signal site (AATAAA) 358-bp downstream of the stop codon (TAA) (Supp Fig. 4 [online only]). Surprisingly, no conventional TATA box was identified in the sequence of the 3′-UTR. The *SeCPR* ORF is 2,070 bp and encodes a putative protein of 690 amino acids with a predicted Mw of 77.7 kDa and a theoretical *pI* of 5.37.

Fig. 1. Nucleotide sequences and deduced amino acid sequences of *Se*CYP9A11 including the 3′- and 5′-UTR. The asterisk indicates the stop codon. The functional regions of *Se*CYP9A11 are identified, boxed, and labeled, and the transmembrane sequences of *Se*CYP9A11 are underlined.

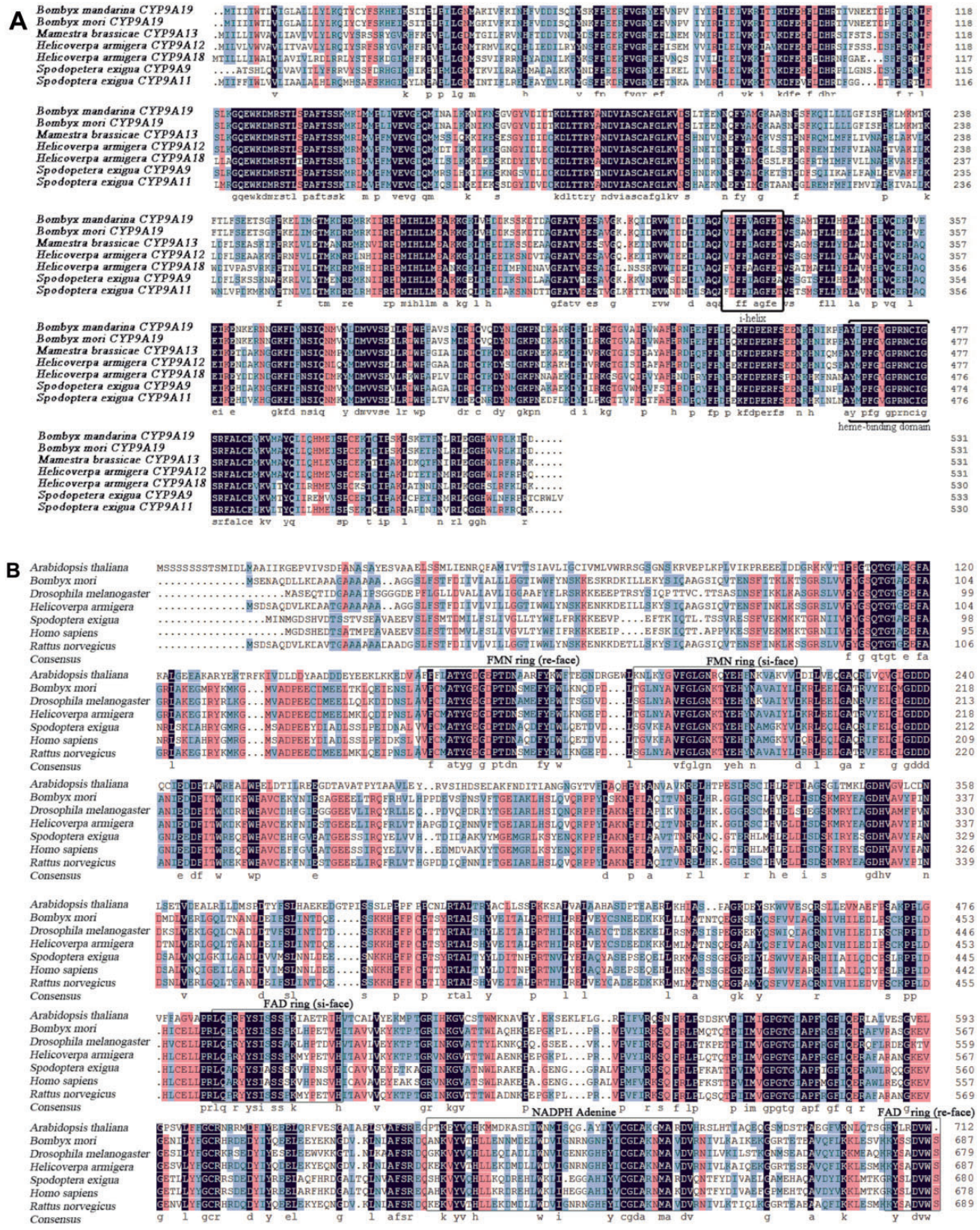

Fig. 2. Comparison of the deduced amino acid sequences of *Se*CYP9A11 with other CYPs (A) and *Se*CPR with other CPRs (B). A, the species names and the GenBank accession numbers are as follows: *B. mandarina CYP9A19* (BAM73827.1), *B. mori CYP9A19* (ABQ08710.1), *M. brassicae CYP9A13* (AAR26518.1), *H. armigera CYP9A12* (AAQ73544.1), *H. armigera CYP9A18* (ABB69055.1), *S. exigua CYP9A9* (ACI43222.1), and *S. exigua CYP9A11* (ADP55210.1). B, *A. thaliana* (CAB58576.1), *B. mori* (NP_001104834.1), *Dr. melanogaster* (AAF52367.1), *H. armigera* (ADK25060.1), *S. exigua* (ADX95746.1), *H. sapiens* (NP_000932.3), and *R. norvegicus* (NP_113764.1).

No signal peptide (Supp Fig. 2B [online only]) was observed within the deduced amino acid sequence of *Se*CPR, though a transmembrane anchor near the *N*-terminus, and the transmembrane domain is composed of 23 amino acid residues from G_{26} to L_{48} (GSLFSTFDIIVLVILLGGTIWWL). The *Se*CPR hydrophobicity diagram was shown in Supp Fig. 3B [online only]. The functional domains, FMN, FAD, and NADPH, which are involved in cofactor binding, are predicted in the primary structure of *Se*CPR (Supp Fig. 4 [online only]). Similar to the conserved motif in other organisms (Ingelman et al. 1997; Zhao et al. 2014), the FAD-binding motif of *Se*CPR consists of three amino acids, Arg 467, Tyr 469, and Ser 470 as well. Meanwhile, the catalytic residues consist of Ser 469, Asp 686, and Try 688 (Supp Fig. 4 [online only]). According to the three-dimensional structure of *Se*CPR (Supp Fig. 5 [online only]), the binding pocket of NADP is composed of 15 amino acids (R 311, V 487, V 489, G 546, T 547, C578, R579, S 607, R 608, K 613,Y 615, T 617, D 643, M 647, D 650), and the binding pocket of FAD is composed of 13 amino acids (H 332, R 467, Y 468, Y 469, S 470, T 485, A 486, V 487, G 501, V 502, T 503, T 504, W 688). At the *N*-terminus, two FMN binding sites are identified in the FMN domain, which possess similar structures to flavodoxins and interact with the redox-partner binding site of CYPs (Lamb et al. 2006). At the *C*-terminus, the identified FAD and NADP binding domains are similar to those in human (*H. sapiens*), *H. armigera* and bed bug (*Cimex lectularius*) (Pandey et al. 2007; Zhu et al. 2012; Zhao et al. 2014).

Of *Se*CPR and other known CPRs on the deduced amino acid sequences level, the alignment results showed that the CPRs in yeast (*Saccharomyces cerevisiae*), thale cress (*Arabidopsis thaliana*), rat (*R. norvegicus*), *H. sapiens*, fruit fly (*Drosophila melanogaster*), *B. mori,* and *H. armigera* shared 30.15, 36.44, 58.5, 54.13, 67.95, 87.48, and 95.21% identity with *Se*CPR, respectively, which confirmed that *Se*CPR is a member of the CPR family. As anticipated, phylogenetic analysis results substantiated that CPRs from the close relationship insect were grouped together (Supp Fig. 6 [online only]).

Temporal and Spatial Expression of SeCYP9A11 and SeCPR mRNA. The temporal and spatial transcription profiles of *SeCYP9A11* and *SeCPR* in different instar larvae, pupa, and adults were determined. The β-actin gene was used as a reference gene to normalize the expression levels of *SeCYP9A11* and *SeCPR* mRNAs, as performed in previous studies (Cheng et al. 1988; Zhu et al. 2013). The results showed that the efficiency and linearity of RT-qPCR assays were sufficient for using β-actin as a reference gene with high confidence level.

The highest expression level of *SeCYP9A11* mRNA was observed in the midgut (Fig. 3A). The expression levels of *SeCYP9A11* mRNA were increased from the 1st to the 5th instar larvae, and the fifth instar larvae and pupae showed the highest and lowest expression levels during the growth, respectively (Fig. 3B).

The expression level of *SeCPR* mRNA in the midgut of the fifth instar larvae were 2.55- and 5.32-fold higher than those in the fat body and cuticle, respectively (Fig. 3C). Significant differences in the

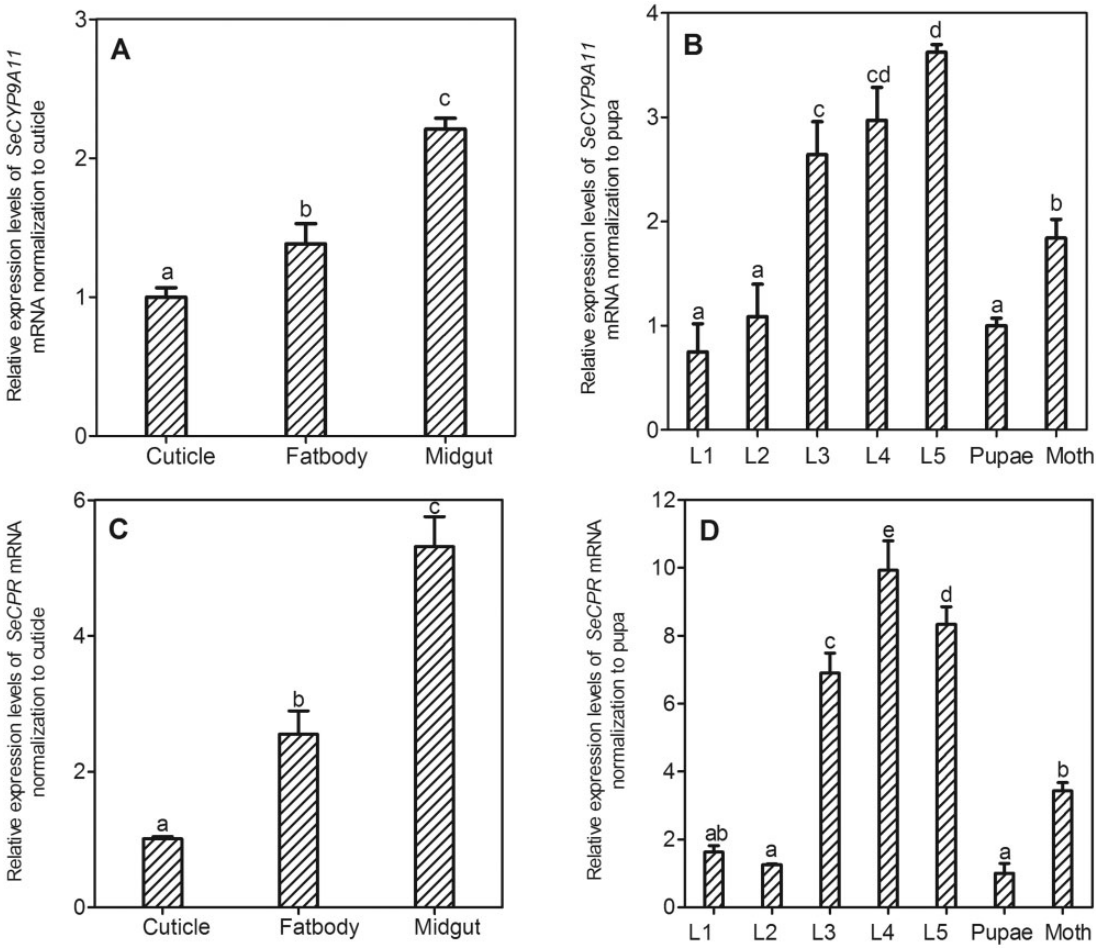

Fig. 3. Relative mRNA expression levels of *S. exigua SeCYP9A11* and *SeCPR* in different tissues of the fifth instar larvae (A and C) and in several development stages including the 1st to 5th instar larvae, pupae and moth (B and D). L1, L2, L3, L4, and L5 indicate the 1st, 2nd, 3rd, 4th, and 5th instar larvae, respectively. Different lower-case letters indicate significant differences based on DMRT, $P < 0.05$. The error bars represent the SEs of triplicates.

expression levels of *SeCPR* mRNA were observed between different development stages, including in larvae from the 1st to 5th instar, pupae, and adult (~2–3 days old) (Fig. 3D). The expression level of *SeCPR* mRNA in the fourth instar was the highest, which was 9.9-fold higher than that in the pupae.

Effects of Quercetin and Tannin on the mRNA Expression Levels of SeCYP9A11 and SeCPR. Treatment with quercetin and tannin has no impact on *S. exigua* mortality. The expression of *SeCYP9A11* mRNA in the midgut of *S. exigua* was significantly inhibited upon dietary exposure to quercetin at doses from 0.1 to 1 mg/g and upon dietary exposure to tannin at doses from 0.5 to 5 mg/g. The expression levels of mRNA decreased by 12.5- and 15.5-fold after 1 mg/g treatment of quercetin and tannin, respectively (Fig. 4A and B).

The *SeCPR* mRNA expression levels were also remarkably inhibited by quercetin (at 0.1 mg/g) and tannin compared with that of the control (Fig. 4C and D).

Discussion

CYP and CPR are the primary components of the cytochrome P450 system that involved the normal metabolism of both endogenous compounds and xenobiotics (Horike et al. 2000; Liu et al. 2013). CPR is an electron donor and shuttles an electron to CYP, which is an essential step in the cytochrome P450 catalytic cycle. To promote the understanding of P450 system in *S. exigua*, a novel CYP member, *SeCYP9A11* gene, and the *SeCPR* gene from *S. exigua* were identified and characterized. The temporal and spatial expression of *SeCYP9A11* and *SeCPR* mRNA, as well as the effects of secondary metabolites from host plants on the mRNA expression of both genes, were investigated in the current study.

The putative protein sequence of *Se*CYP9A11 exhibited a heme-binding domain and a characteristic conserved sequence specific to the CYP9 family (SRFALCE) (Fig. 1). The signal peptide that may be responsible for directing *Se*CYP9A11 to the periplasmic space in cells and the transmembrane segment at the *N*-terminal end region of *Se*CYP9A11 were predicted. Alignment analysis revealed that *Se*CYP9A11 shared the highest sequence similarity with *Mb*CYP9A13 from *M. brassicae*, with a protein-sequence identity of 66.54% (Fig. 2A).

The conserved polyadenylation signal (AATAAA) nucleotide sequence of *SeCPR* is consistent with most other CPRs in eukaryotes (Guo and Sherman 1996; Zhao et al. 2014). No conserved signal peptide was found at the *N*-terminal end of *Se*CPR, suggesting that *Se*CPR may be retained in the cytoplasm (Supp Fig. 3 [online only]). Meanwhile, CPR is typically anchored in the endoplasmic reticulum (ER) membrane by the *N*-terminal hydrophobic segment, which is essential for CPR function in P450 catalytic metabolism (Kida et al. 1998; Zhu et al. 2012). The *Se*CPR is predicted to harbor a transmembrane region at the *N*-terminal end, which may be responsible for the remainder of the *Se*CPR enzyme to face the cytoplasmic side of the membrane (Sanglard et al. 1993). For electron transfer, maintaining the proper spatial interactions between CPR and CYP is important, that is mediated by the protein anchored to the ER (Wang et al. 1997; Pandey

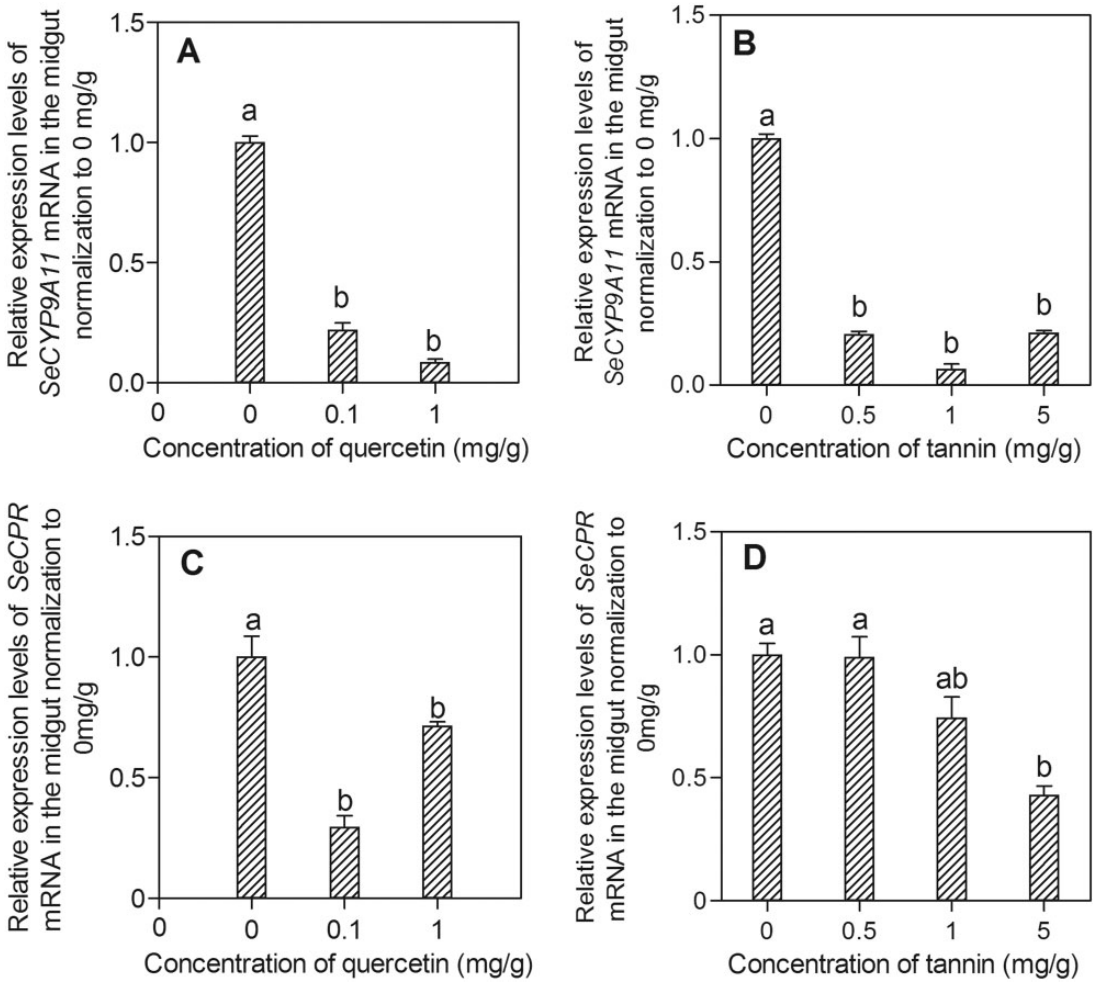

Fig. 4. Relative expression levels of *SeCYP9A11* and *SeCPR* mRNA in the midgut of fourth instar larvae treated with quercetin (A and C) or tannin (B and D) at 48 h. Different lower-case letters indicate significant differences ($P < 0.05$) based on DMRT comparing with the control. The error bars represent the SEs of three replicates.

et al. 2007) and the similar results have been documented for *C. lectularius, Chilo suppressalis,* and *H. armigera* (Zhu et al. 2012; Liu et al. 2013; Liu et al. 2014; Zhao et al. 2014). The high level of homology between *Se*CPR and *Ha*CPR may be due to the close evolutionary relationship of *S. exigua* and *H. armigera*, as both belong to the Noctuidae insect family (Zhao et al. 2014). The primary structures of the CPRs are highly conserved across diverse taxa, indicating the functional importance of this enzyme throughout insect evolution (Wang et al. 1997).

The putative structure of CPR consists of the FMN-, FAD-, and NADP-binding domains and the catalytic residues. As the catalytic cycle continues, the CPR transfers a hydride ion from NADPH to FMN due to the lower redox potential of FAD, and the hydride electron is then delivered to acceptor proteins such as CYPs (Vermilion et al. 1981; Oprian and Coon 1982) to activate molecular oxygen (Nebert and Gonzalez 1987), Cyt-b_5 (Enoch and Strittmatter 1979), heme oxygenase (Schacter et al. 1972), squalene epoxidase (Teruo et al. 1977), and fatty acid elongase (Ilan et al. 1981). Furthermore, the catalytic residues (Supp Fig. 4 [online only]) are crucial for the hydride transfer catalyzed by the rat CYP oxidoreductase (Shen et al. 1999; Hubbard et al. 2001). At the *N*-terminus, the FMN-binding domain consists of the two FMN-binding sites FMN1 and FMN2. These binding sites are highly conserved among all insect CPRs, indicating that they may play key roles in the interaction between CPR and CYP (Zhu et al. 2012). Lamb et al. (2006) has reported that mutation of D187A and T71A in the *S. cerevisiae* CPR FMN-binding site almost completely destroys the functional activity involving CYP51.

Many previous studies have shown that CYP and CPR are expressed throughout life stages and are distributed in various tissues in insects (Ranasinghe and Hobbs 1999; Maïbèche-Coisne et al. 2005; Zhang et al. 2010; Liu et al. 2014). These conclusions were further confirmed in our study. The transcripts of *SeCYP9A11* and *SeCPR* were detected in all of the tested tissues (midgut, fat body, and cuticle) and throughout all developmental stages, from first instar larvae to the adults of *S. exigua*. As we known, CYP and CPR play important roles in the metabolism of plant natural products (Wang et al. 2001; Foster et al. 2003; Seki et al. 2008; Riddick et al. 2013). Hence, the temporal tissue distribution of *CPR* and *CYP* mRNA may be associated with the location of xenobiotic metabolism. In this study, much higher expression levels of *SeCPR* and *SeCYP9A11* mRNA were observed in the midgut compared with that in the fat body and cuticle, suggesting midgut is the most important part of digestive system in *S. exigua*.

Quercetin and tannin have frequently been used to study the induction of CYP in insects and mammals (Tsyrlov et al. 1994; Rahden-Staron et al. 2001). However, information regarding the expression of *SeCYP9A11* and *SeCPR* mRNA after treatment with quercetin and tannin is unavailable. In this study, the *SeCYP9A11* and *SeCPR* mRNA expression levels were inhibited mostly in the midgut of fourth instar larvae after treating with quercetin ($\leq$1 mg/g) and tannin ($\leq$5 mg/g). This result is in agreement with those of earlier reports (Krajka-Kuźniak and Baer-Dubowska 2003; Yao et al. 2008; Liu et al. 2014; Rastogi and Jana 2014). Yao et al. (2008) reported that tannic acid preferably inhibits the activity of human CYP1A2 as well as CPR and concluded that the inhibition of CYP activity by tannic acid may partially be due to the inhibition of CPR activity. Liu et al. (2014) also observed that tannic acid and quercetin have inhibitory effects on CPR activity with IC_{50} values ranging from 15 to 90 μM.

In conclusion, two novel genes (*SeCYP9A11* and *SeCPR*) of *S. exigua* cytochrome P450 system were cloned and characterized, and the putative functions of both genes were assessed. Previous studies have suggested that the identification of *CYP* and *CPR* genes in insects may function as biomarkers of insecticides to reveal the mechanism of pesticide resistance (Lycett et al. 2006; Lian et al. 2011). However, further study is required to determine the other physiological processes of *SeCYP9A11* to *SeCPR* in *S. exigua*, and perhaps in insecticide-resistant populations.

Supplementary Data

Supplementary data are available at *Journal of Insect Science* online.

Acknowledgment

This study was supported by the National Natural Science Foundation of China (Grant No. 30971943).

References Cited

Atkins, L. E., Jr. 1960. The beet armyworm, *Spodoptera exigua*, an economic pest of citrus in California. J. Econ. Entomol. 53: 616–619.

Bergé, J. B., R. Feyereisen, and M. Amichot. 1998. Cytochrome P450 monooxygenases and insecticide resistance in insects. Philos. T. Roy. Soc. B 353: 1701–1705.

Che, W., T. Shi, Y. Wu, and Y. Yang. 2013. Insecticide resistance status of field populations of *Spodoptera exigua* (Lepidoptera: Noctuidae) from China. J. Econ. Entomol. 106: 1855–1862.

Cheng, E., W. Lu, W. Lin, D. Lin, and T. Tsai. 1988. Effective control of beet armyworm, *Spodoptera exigua* (Hübner), on green onion by the ovicidal action of bifenthrin. J. Agric. Res. China 37: 320–327.

Enoch, H. G., and P. Strittmatter. 1979. Cytochrome b5 reduction by NADPH-cytochrome P-450 reductase. J. Biol. Chem. 254: 8976–8981.

Feyereisen, R. 2012. Insect CYP genes and P450 enzymes. Chapter 8. pp. 236–316. *In* L. I. Gilbert (ed.), Insect Molecular Biology and Biochemistry. Academic Press, San Diego, CA.

Foster, B. C., S. Vandenhoek, J. Hana, A. Krantis, M. H. Akhtar, M. Bryan, J. W. Budzinski, A. Ramputh, and J. T. Arnason. 2003. *In vitro* inhibition of human cytochrome P450-mediated metabolism of marker substrates by natural products. Phytomedicine 10: 334–342.

Gasteiger, E., C. Hoogland, A. Gattiker, S. Duvaud, M. Wilkins, R. Appel, and A. Bairoch. 2005a. Protein identification and analysis tools on the ExPASy Server, pp. 571–607. *In* J. Walker (ed.), The Proteomics Protocols Handbook. Humana Press, Totowa, NJ.

Guo, Z., and F. Sherman. 1996. Signals sufficient for 3′-end formation of yeast mRNA. Mol. Cell. Biol. 16: 2772–2776.

Horike, N., H. Takemori, Y. Nonaka, H. Sonobe, and M. Okamoto. 2000. Molecular cloning of NADPH-cytochrome P450 oxidoreductase from silkworm eggs. Eur. J. Biochem. 267: 6914–6920.

Hubbard, P. A., A. L. Shen, R. Paschke, C. B. Kasper, and J.-J.P. Kim. 2001. NADPH-cytochrome P450 oxidoreductase. Structural basis for hydride and electron transfer. J. Biol. Chem. 276: 29163–29170.

Ilan, Z., R. Ilan, and D. L. Cinti. 1981. Evidence for a new physiological role of hepatic NADPH:ferricytochrome (P-450) oxidoreductase. Direct electron input to the microsomal fatty acid chain elongation system. J. Biol. Chem. 256: 10066–10072.

Ingelman, M., V. Bianchi, and H. Eklund. 1997. The three-dimensional structure of flavodoxin reductase from *Escherichia coli* at 1.7 å resolution. J. Mol. Biol. 268: 147–157.

Kelley, L. A., and M.J.E. Sternberg. 2009. Protein structure prediction on the Web: a case study using the Phyre server. Nat. Protoc. 4: 363–371.

Kida, Y., S. Ohgiya, K. Mihara, and M. Sakaguchi. 1998. Membrane topology of NADPH–cytochrome P450 reductase on the endoplasmic reticulum. Arch. Biochem. Biophys. 351: 175–179.

Konus, M., C. Koy, S. Mikkat, M. Kreutzer, R. Zimmermann, M. Iscan, and M. O. Glocker. 2013. Molecular adaptations of *Helicoverpa armigera* midgut tissue under pyrethroid insecticide stress characterized by differential proteome analysis and enzyme activity assays. Comp. Biochem. Physiol. D: Genomics Proteomics 8: 152–162.

Krajka-Kuźniak, V., and W. Baer-Dubowska. 2003. The effects of tannic acid on cytochrome P450 and phase II enzymes in mouse liver and kidney. Toxicol. Lett. 143: 209–216.

Krogh, A., B. Larsson, G. von Heijne, and E.L.L. Sonnhammer. 2001. Predicting transmembrane protein topology with a hidden markov model: application to complete genomes. J. Mol. Biol. 305: 567–580.

Lamb, D. C., Y. Kim, L. V. Yermalitskaya, V. N. Yermalitsky, G. I. Lepesheva, S. L. Kelly, M. R. Waterman, and L. M. Podust. 2006. A second FMN binding site in yeast NADPH-cytochrome P450 reductase suggests a mechanism of electron transfer by diflavin reductases. Structure 14: 51–61.

Lian, L.-Y., P. Widdowson, L. A. McLaughlin, and M.J.I. Paine. 2011. Biochemical comparison of *Anopheles gambiae* and human NADPH P450 reductases reveals different 2′-5′-ADP and FMN binding traits. PLoS One 6: e20574.

Liu, D., X. Zhou, M. Li, S. Zhu, and X. Qiu. 2014. Characterization of NADPH–cytochrome P450 reductase gene from the cotton bollworm, *Helicoverpa armigera*. Gene 545: 262–270.

Liu, S., Q. M. Liang, Y. J. Huang, X. Yuan, W. W. Zhou, F. Qiao, J. Cheng, G. M. Gurr, and Z. R. Zhu. 2013. Cloning, functional characterization, and expression profiles of NADPH-cytochrome P450 reductase gene from the Asiatic rice striped stem borer, *Chilo suppressalis* (Lepidoptera: Pyralidae). Comp. Biochem. Physiol. B. Biochem. Mol. Biol. 166: 225–231.

Livak, K. 2001. Analysis of relative gene expression data using real-time quantitative PCR and the $2^{-\Delta\Delta CT}$ method. Methods. 25: 402–408.

Lycett, G. J., L. A. McLaughlin, H. Ranson, J. Hemingway, F. C. Kafatos, T. G. Loukeris, and M.J.I. Paine. 2006. *Anopheles gambiae* P450 reductase is highly expressed in oenocytes and *in vivo* knockdown increases permethrin susceptibility. Insect Mol. Biol. 15: 321–327.

Maïbèche-Coisne, M., C. Merlin, M.-C. François, P. Porcheron, and E. Jacquin-Joly. 2005. P450 and P450 reductase cDNAs from the moth *Mamestra brassicae*: cloning and expression patterns in male antennae. Gene 346: 195–203.

Mao, W., S. Rupasinghe, A. R. Zangerl, M. A. Schuler, and M. R. Berenbaum. 2006. Remarkable substrate-specificity of CYP6AB3 in *Depressaria pastinacella*, a highly specialized caterpillar. Insect Mol. Biol. 15: 169–179.

Marchler-Bauer, A., S. Lu, J. B. Anderson, F. Chitsaz, M. K. Derbyshire, C. DeWeese-Scott, J. H. Fong, L. Y. Geer, R. C. Geer, N. R. Gonzales et al. 2011. CDD: a conserved domain database for the functional annotation of proteins. Nucleic Acids Res. 39: 225–229.

Mohaghegh, J., P. D. Clercq, and L. Tirry. 2001. Functional response of the predators *Podisus maculiventris* (Say) and *Podisus nigrispinus* (Dallas) (Het., Pentatomidae) to the beet armyworm, *Spodoptera exigua* (Hübner) (Lep., Noctuidae): effect of temperature. J. Appl. Entomol. 125: 131–134.

Murataliev, M. B., V. M. Guzov, F. A. Walker, and R. Feyereisen. 2008. P450 reductase and cytochrome b_5 interactions with cytochrome P450: effects on house fly CYP6A1 catalysis. Insect Biochem. Mol. Biol. 38: 1008–1015.

Nebert, D. W., and F. J. Gonzalez. 1987. P450 genes: structure, evolution, and regulation. Annu. Rev. Biochem. 56: 945–993.

Oprian, D. D., and M. J. Coon. 1982. Oxidation-reduction states of FMN and FAD in NADPH-cytochrome P450 reductase during reduction by NADPH. J. Biol. Chem. 257: 8935–8944.

Pandey, A. V., P. Kempná, G. Hofer, P. E. Mullis, and C. E. Flück. 2007. Modulation of human CYP19A1 activity by mutant NADPH P450 oxidoreductase. Mol. Endocrinol. 21: 2579–2595.

Park, J., J. Lee, W. Lee, H. Goh, and K. Kim. 1991. Flight activity and injury characteristics of beet armyworm, *Spodoptera exigua* (Hübner), (Lepidoptera: Noctuidae) in southern region of Korea. Korean J. Appl. Entomol. 30: 124–129.

Petersen, T. N., S. Brunak, G. von Heijne, and H. Nielsen. 2011. SignalP 4.0: discriminating signal peptides from transmembrane regions. Nat. Methods 8: 785–786.

Pettersen, E. F., T. D. Goddard, C. C. Huang, G. S. Couch, D. M. Greenblatt, E. C. Meng, and T. E. Ferrin. 2004. UCSF Chimera - a visualization system for exploratory research and analysis. J. Comput. Chem. 25: 1605–1612.

Pompon, D., B. Louerat, A. Bronine, and P. Urban. 1996. Yeast expression of animal and plant P450s in optimized redox environments, 272: pp. 51–64. *In* F. J. Eric, R. W. Michael (eds.), Methods Enzymol. Academic Press, San Diego, CA.

Rahden-Staron, I., H. Czeczot, and M. Szumilo. 2001. Induction of rat liver cytochrome P450 isoenzymes CYP 1A and CYP 2B by different fungicides, nitrofurans, and quercetin. Mutat. Res. 498: 57–66.

Ranasinghe, C., and A. A. Hobbs. 1999. Induction of cytochrome P450 *CYP6B7* and cytochrome b_5 mRNAs from *Helicoverpa armigera* (Hübner) by pyrethroid insecticides in organ culture. Insect Mol. Biol. 8: 443–447.

Rastogi, H., and S. Jana. 2014. Evaluation of inhibitory effects of caffeic acid and quercetin on human liver cytochrome P450 activities. Phytother. Res. 28: 1873–1878.

Riddick, D. S., X. Ding, C. R. Wolf., T. D. Porter, A. V. Pandey, Q.-Y. Zhang, J. Gu, R. D. Finn, S. Ronseaux, L. A. McLaughlin, et al. 2013. NADPH–cytochrome P450 oxidoreductase: roles in physiology, pharmacology, and toxicology. Drug Metab. Dispos. 41: 12–23.

Ruberson, J. R., G. A. Herzog, W. R. Lambert, and W. J. Lewis. 1994. Management of the beet armyworm (Lepidoptera: Noctuidae) in cotton: role of natural enemies. Fla. Entomol. 77: 440–453.

Sanglard, D., C. Sengstag, and W. Seghezzi. 1993. Probing the membrane topology of *Candida tropicalis* cytochrome P450. Eur. J. Biochem. 216: 477–485.

Schacter, B. A., E. B. Nelson, H. S. Marver, and B.S.S. Masters. 1972. Immunochemical evidence for an association of heme oxygenase with the microsomal electron transport system. J. Biol. Chem. 247: 3601–3607.

Scott, J. G. 1999. Cytochromes P450 and insecticide resistance. Insect Biochem. Mol. Biol. 29: 757–777.

Scott, J. G., N. Liu, and Z. M. Wen. 1998. Insect cytochromes P450: diversity, insecticide resistance and tolerance to plant toxins. Comp. Biochem. Physiol. C, Pharmacol. Toxicol. Endocrinol. 121: 147–155.

Seki, H., K. Ohyama, S. Sawai, M. Mizutani, T. Ohnishi, H. Sudo, T. Akashi, T. Aoki, K. Saito, and T. Muranaka. 2008. Licorice β-amyrin 11-oxidase, a cytochrome P450 with a key role in the biosynthesis of the triterpene sweetener glycyrrhizin. Proc. Natl. Acad. Sci. U. S. A. 105: 14204–14209.

Shen, A. L., D. S. Sem, and C. B. Kasper. 1999. Mechanistic studies on the reductive half-reaction of NADPH-cytochrome P450 oxidoreductase. J. Biol. Chem. 274: 5391–5398.

Tamura, K., D. Peterson, N. Peterson, G. Stecher, M. Nei, and S. Kumar. 2011. MEGA5: molecular evolutionary genetics analysis using maximum likelihood, evolutionary distance, and maximum parsimony methods. Mol. Biol. Evol. 28: 2731–2739.

Teruo, O., O. Shigeru, H. Fumihiko, and I. Yoh. 1977. Involvement of NADPH-cytochrome c reductase in the rat liver squalene epoxidase system. Biochim. Biophys. Acta. 486: 401–407.

Tsyrlov, I. B., V. M. Mikhailenko, and H. V. Gelboin. 1994. Isozyme- and species-specific susceptibility of cDNA-expressed CYP1A *P*-450s to different flavonoids. Biochim. Biophys. Acta. 1205: 325–335.

Vermilion, J. L., D. P. Ballou, V. Massey, and M. J. Coon. 1981. Separate roles for FMN and FAD in catalysis by liver microsomal NADPH-cytochrome P-450 reductase. J. Biol. Chem. 256: 266–277.

Wang, E., R. Wang, J. DeParasis, J. H. Loughrin, S. Gan, and G. J. Wagner. 2001. Suppression of a P450 hydroxylase gene in plant trichome glands enhances natural-product-based aphid resistance. Nat. Biotechnol. 19: 371–374.

Wang, M., D. L. Roberts, R. Paschke, T. M. Shea, B.S.S. Masters, and J.-J.P. Kim. 1997. Three-dimensional structure of NADPH–cytochrome P450 reductase: prototype for FMN- and FAD-containing enzymes. Proc. Natl. Acad. Sci. U. S. A. 94: 8411–8416.

Wen, Z., L. Pan, M. R. Berenbaum, and M. A. Schuler. 2003. Metabolism of linear and angular furanocoumarins by *Papilio polyxenes* CYP6B1 coexpressed with NADPH cytochrome P450 reductase. Insect Biochem. Mol. Biol. 33: 937–947.

Yang, J., R. Yan, A. Roy, D. Xu, J. Poisson, and Y. Zhang. 2015. The I-TASSER Suite: protein structure and function prediction. Nat. Methods 12: 7–8.

Yao, H.-T., Y.-W. Chang, S.-J. Lan, and T.-K. Yeh. 2008. The inhibitory effect of tannic acid on cytochrome P450 enzymes and NADPH-CYP reductase in rat and human liver microsomes. Food Chem. Toxicol. 46: 645–653.

Zhang, H., T. Tang, Y. Cheng, R. Shui, W. Zhang, and L. Qiu. 2010. Cloning and expression of cytochrome P450 *CYP6B7* in fenvalerate-resistant and susceptible *Helicoverpa armigera* (Hübner) from China. J. Appl. Entomol. 134: 754–761.

Zhao, C., T. Tang, X. Feng, and L. Qiu. 2014. Cloning and characterisation of NADPH-dependent cytochrome P450 reductase gene in the cotton bollworm, *Helicoverpa armigera*. Pest Manag. Sci. 70: 130–139.

Zhu, F., S. Sams, T. Moural, K. F. Haynes, M. F. Potter, and S. R. Palli. 2012. RNA interference of NADPH-Cytochrome P450 reductase results in reduced insecticide resistance in the bed bug, *Cimex lectularius*. PLoS One 7: e31037.

Zhu, J., L. Zhang, S. Ze, D. Wang, and B. Yang. 2013. Identification and tissue distribution of odorant binding protein genes in the beet armyworm, *Spodoptera exigua*. J. Insect Physiol. 5: 722–728.

Received 12 June 2015; accepted 3 August 2015.